

Does the center of resistance depend on the direction of tooth movement?

Brandon N. Meyer,^a Jie Chen,^b and Thomas R. Katona^c

Indianapolis, Ind

Introduction: The objective of this study was to compare the locations of the centers of resistance (CRes) in the buccolingual (BL) and mesiodistal (MD) directions of the mandibular central incisors of 6 dogs. **Methods:** Based on microcomputed tomography images of the teeth and their supporting tissues, solid models were used to build finite element models. **Results:** The CRes locations for the 6 specimens were determined for displacements in the BL and MD directions with finite element calculations. Measured from the alveolar crest, the BL and MD locations were 43% to 51% and 31% to 43% of root length, respectively. Their average locations, 46.2% and 38.3%, were statistically different at the 95% CI. **Conclusions:** The CRes location for BL tooth movement is significantly more apical than its MD counterpart. (Am J Orthod Dentofacial Orthop 2010;137:354-61)

Orthodontic tooth displacement is described as translation, rotation, or a combination thereof. Any such movement can be characterized by its associated center of rotation (CRot).¹ Clinically, the displacement has been described in 2-dimensional planes. In each plane, the orthodontic load (force and moment) system required to achieve a desired displacement depends on the position of the tooth's center of resistance (CRes). Its location is a function of root and supporting structure anatomy, and their mechanical properties.² The most popular definition of CRes, a powerful conceptual tool, is the point, fixed relative to the root, that, if a force were applied to it, the tooth would undergo pure translation. An alternate definition is the point about which the tooth would rotate if only a moment of a couple were applied (anywhere) to the tooth. Clinically, the distance between the CRes and the bracket is equal to the moment-to-force ratio (M/F) required of a loop for tooth translation, and the amount of tooth tipping and root correction can be controlled by deviating from that ratio.

Experimental and analytical methods were used to locate the CRes.³⁻¹⁴ For example, Yoshida et al¹⁴ used

a magnetic sensing system to demonstrate that in-vivo central-incisor CRes locations were influenced by bone height. Matsui et al⁵ used a photoelastic model to study the CRes of the anterior arch segment. However, most studies were based on simplified idealized finite element (FE) models in which CRes locations of specific teeth were reported.^{2-4,6,7,10,12,13,15,16} A 2-dimensional mathematical model was used to show that the most occlusal and apical CRes locations correspond to triangular and rectangular root shapes, respectively.¹¹ A root-like shape produced a more apically located CRes than was experimentally measured by Yoshida et al¹⁴ but close to the location reported by Christiansen and Burstone.¹² These results indicate that the more tapered the root, the more occlusal the CRes. Vollmer et al¹³ compared idealized and realistic 3-dimensional (3D) root anatomies and found that the latter produced a CRes location that was consistent with many other groups' findings, but it was more apical than predicted by their more tapered idealized root. This trend seems reasonable because the apical root region cross-sectional area decreases with more taper and, thus, produces relatively less resistance to root motion near the apex. In general, analytical and experimental studies have indicated that the CRes of a single-rooted tooth is somewhere in the middle third of its root.^{2-4,14} However, it has not been reported whether a tooth has a single CRes or whether the CRes also depends on the direction of displacement.

Because it forms the compliant structure that supports the tooth, the periodontal ligament (PDL) is the primary determinant of the CRes location. FE models of the bone-PDL-tooth complex have been used to study the stresses in the complex and tooth movement.^{2-4,6,7,10,12,13,15-17} Thus far, however, only 2

From Indiana University Purdue University Indianapolis, Indianapolis, Ind.

^aPostgraduate student, Department of Mechanical Engineering and Department of Orthodontics and Oral Facial Genetics.

^bProfessor, Department of Mechanical Engineering.

^cAssociate professor, Department of Orthodontics and Oral Facial Genetics and Department of Mechanical Engineering.

Supported by NIH-NIDCR R41-DE017025 and R01-DE015767.

The authors report no commercial, proprietary, or financial interest in the products or companies described in this article.

Reprint requests to: Jie Chen, Department of Mechanical Engineering, Indiana University Purdue University, 723 W. Michigan Street, Indianapolis, IN 46202; e-mail, jchen3@iupui.edu.

Submitted, December 2007; revised and accepted, March 2008.

0889-5406/\$36.00

Copyright © 2010 by the American Association of Orthodontists.

doi:10.1016/j.ajodo.2008.03.029

articles have shown the PDL as a structurally realistic tension-only fiber-reinforced matrix.^{16,17} Provatidis¹⁷ did not directly address CRes location but found that it depended on fiber volume concentration when fiber angulations were not varied. Qian et al¹⁶ showed that the inclusion of fibers in the PDL model was an important determinant of CRes and CRot locations, although fiber orientation and stiffness, within reasonable ranges, had relatively little influence.

No study has compared buccolingual (BL) with mesiodistal (MD) CRes locations, and more realistic models are needed. Thus, the main objectives of this 3D FE study were to improve on the previously reported model and to investigate the effects of orthodontic load direction on the CRes of anatomically correct dog teeth.¹⁶

MATERIAL AND METHODS

Six mandibular central incisors and their supporting tissues (PDL and alveolar bone) were obtained from 6 dogs that had been killed for an unrelated project. The specimens were scanned in a micocomputed tomography (μ CT) unit (model 1072, SkyScan, Kontich, Belgium) to form the bases for 3D FE models. MIMICS software (version 9.0, Materialise, Leuven, Belgium) and Unigraphics NX (Siemens, Plano, Tex) were used to convert the μ CT images into solid models as follows. For a tooth with a root approximately 12 mm long, 70 sections were selected along its long axis to assess the root, PDL, and alveolar bone. With MIMICS, the PDL and root boundaries in each section were demarcated by contour lines based on gray value threshold regions (Fig 1). An IGES file of each structure's contour was created and loaded into Unigraphics to convert them into solid structures. Depending on the anatomic complexity of the root and the PDL, 10 of the 70 sets of contour lines were selected for the model. A set of 20 equidistant points on each line was made, and second-order interpolation curve fitting was performed to smooth the contour. The solid structures of the PDL and the root were constructed from the resulting smoothed contours. A uniform cortical bone "shell" (lamina dura) was created around the PDL by offsetting the PDL contours. The process is shown in Figure 1.

The solid model was imported into ANSYS software (version 10.0, ANSYS, Canonsburg, Pa) for assembly, meshing, and analysis. The bone, PDL matrix, and tooth were meshed with 10-node tetrahedral (SOLID187) elements. An atypical feature of the model is the incorporation of tension-only 3D spar (LINK10) elements to represent the principal fibers of the PDL. To create the fibers, a program was written to produce an ANSYS macro file that generated radially projecting

fibers from root nodes to bone-socket nodes, randomly oriented between 20° and 30° to the horizontal, with a relatively even distribution within that range (Table I).¹⁶ In the apical region, the fibers were nearly vertical (Fig 2). This amounts to the modeling of the PDL as a composite material that consists of a fiber-reinforced matrix.

Material properties (Table II) and fiber characterizations (Table III) were obtained from the literature.^{16,18} As is common practice, bone and root were idealized as homogeneous and linear elastic. This is justifiable because, compared with the PDL, the bone and root elastic moduli are several orders of magnitude greater. On the other hand, PDL structural verisimilitude was maintained to the extent possible. In previous studies, particularly those with idealized models, PDL thickness was assumed to be uniform, but it is clear that PDL width varies not only from tooth to tooth, but also within each tooth—a variation that is incorporated in this model (Fig 3).^{2,13,16,17,19}

Each model consisted of an actual root shape and its specific PDL thickness. Because bone and crown have negligible effects on tooth displacement, they were simplified. Each model consisted of a homogeneous tooth (entirely dentin), a fiber-reinforced PDL matrix, and alveolar bone (cancellous bone encased in a thin layer of cortical bone). Zero displacements at the bottom, mesial, and distal sides of the alveolar bone were applied as the boundary conditions. The FE models contained approximately 100,000 elements and 115,000 nodes. Because of nonlinear fiber properties and the large strains experienced by the relatively soft PDL tissues, nonlinear static analyses were performed.

The unknown distance of CRes from the known line of action of the applied force (F) is equal to the required M/F for pure translation of the tooth. A Cartesian coordinate system was created. Its origin was located at the crown, where the force acted with its positive x-axis directed buccally, its y-axis mesially, and its z-axis occlusally. With this coordinate system definition, for the BL (first order) and the MD (second order) displacements, the relevant M/F ratios are M_y/F_x and M_x/F_y , respectively (Fig 4). Based on these principles, the locations of CRes were calculated by using a parametric approach. For the BL direction, a lingually tipping force ($F_x = -1.0$ N) and an incrementally increasing correction moment ($M_y = -1.0, -2.0, -3.0 \dots$ N-mm, or equivalently, $M_y/F_x = 1.0, 2.0, 3.0 \dots$) to counter the moment produced by F_x about the CRes were applied to the buccal sides of the crowns. The sought M_y/F_x produced tooth translation. The same procedure, but with $F_y (= +1.0$ N) and $M_x (= -1.0, -2.0, -3.0 \dots$ N-mm) was performed in the MD direction. But, in contrast to the BL

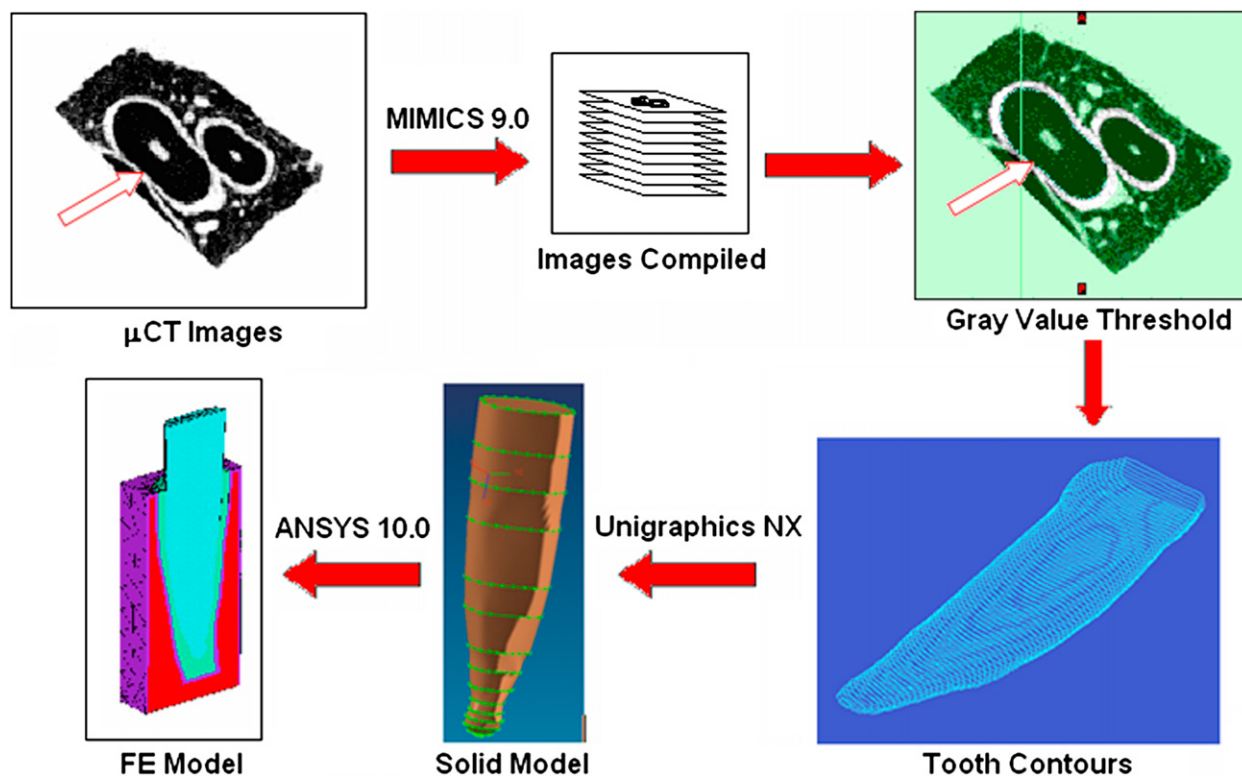


Fig 1. Modeling process of μCT scans to FE model.

Table I. PDL fiber distribution in a specimen

Angle (°)	Elements (n)
20-22	1711
22-24	1476
24-26	1320
26-28	1327
28-30	1381
Apical	321
Total	7536

movement, the line of action of the distally directed $F_y = +1.0$ N force (also applied to the buccal surfaces of the crowns) did not pass through the long axes of the teeth, thereby producing a confounding (+Mz) moment that rotated the teeth along their long axes. This third-order rotation was minimized with the application of a counter-rotating couple, $M_z = -F_c \times d$ N-mm (green arrows in Fig 4), with $F_c = 1.0$ N and d equal to the distance between the root's centerline and the line of action of F_y .

To define tooth translation for those calculations, tooth movement was characterized by a path that was created between a central node on the cervical end of the root and a central node at the root apex. By plotting

path movement in the loading direction for each M/F, the translation-producing M/F could be isolated. In some instances, the appropriate M/F was calculated by interpolation.

RESULTS

The CRes and, as a byproduct, the CRot for each specimen were determined in the BL and MD directions by using the FE results. For illustration, the BL and MD displacement profiles for 1 specimen are shown in Figure 5. The vertical axis represents the distance measured from the line of action of the (1.0 N) orthodontic force on the crown ($y = 0$), approximately 2 mm above the alveolar crest and 1.25 mm from the incisal edge, down to the root apex ($y \approx -12.2$ mm).

The point of intersection of a displacement curve with the vertical axis approximates the location of CRot that corresponds to that specific M/F. As CRot approaches infinity, the displacement curve approaches parallelism with the y-axis. This represents pure translation, and the associated M/F ratio is the M/F required for tooth translation.

The horizontal location of the point of intersection of all M/F curves demarcates the horizontal

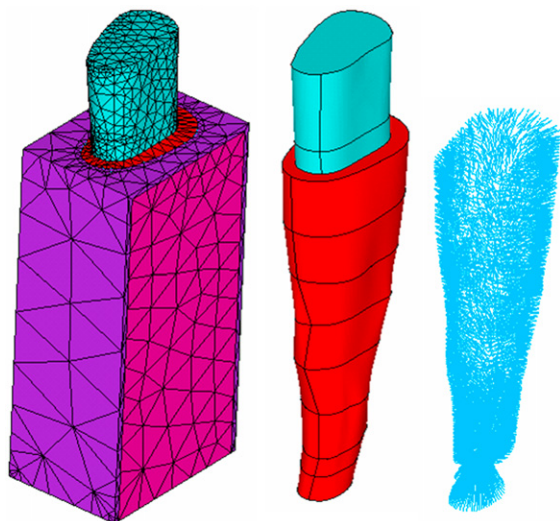


Fig 2. An FE model with randomly oriented PDL fibers: left to right, the complete model, the tooth with the PDL, and the PDL fibers only.

Table II. Material properties

Structure	Elastic modulus (E)	Poisson's ratio (ν)
Alveolar bone		
Cortical	13 GPa	0.30
Cancellous	1 GPa	0.30
Root		
Dentin	18 GPa	0.30
PDL		
Matrix	0.5 MPa	0.47
Fiber	10 MPa	0.35

E, Young's modulus; ν, Poisson's ratio.
Material properties according to Qian et al.¹⁶

displacement of CRes. Corresponding to the 1.0 N orthodontic forces, for this tooth, the BL and MD displacements of CRes are 0.0036 and 0.0026 mm, respectively. Table IV shows CRes translations for all teeth.

The calculated relative locations of CRes, their averages, and standard deviations are also listed in Table IV. For this tooth, the BL movement-associated CRes is about 7.0 mm from the bracket, or M/F = 6.8 mm. The corresponding values for MD movement are about 6.2 mm. Rather than as an absolute distance from the bracket, as in this example, the location of CRes is often measured from the alveolar crest as a percentage of root length. For this tooth, the BL and MD values are 46% and 40%, respectively. For the 6 specimens, from the alveolar crest, the CRes in the BL and MD directions

Table III. PDL fiber density and diameter

Region	Fiber density (fibers/100 μm)	Fiber diameter (μm)
Coronal and middle	22.1	3.4
Apical	13.2	4.6

PDL properties according to Auyeung et al.¹⁸

ranged from 43% to 51% and 31% to 43% of their root lengths, respectively. Their average locations, 46% and 38%, were statistically different at the 95% CI.

DISCUSSION

Evidence-based orthodontic forces and moments that produce specified tooth movements must be predicated on the location of CRes. Clinically, these tooth displacements and orthodontic loads occur in all 3 directions of space, yet most published CRes position models are unidirectional, primarily in the MD direction.²⁰ This FE project localized the CRes for BL and MD movements of 6 dog incisors. Although our computed results are consistent with most previously reported CRes locations—34% to 64% of root length from the alveolar crest—our results also show a statistically significant difference between the locations of CRes in the 2 directions. Furthermore, we found a range of locations even among our 6 similar specimens.

The locations of CRes in the 2 directions differ for a variety of reasons, but most likely because the root is wider in the BL direction than in the MD direction. The results show that the wider the root, the less the force-produced displacement and tipping. Less tipping requires smaller uprighting correction moments, indicating that the location of CRes is more occlusal. These observations, based on actual (dog) root anatomies, were similar to those reported with idealized rectangular and triangular root shapes.^{11,14,17}

The average relative location of CRes (46% of root length from the alveolar crest) for BL movement is more apical than its MD counterpart (38%). It can therefore be concluded that the average, or a specific, canine incisor requires a higher My/Fx for BL translation than Mx/Fy for MD translation. However, when comparing teeth, a clear distinction must be made between the relative and absolute locations of CRes, the 2 ways in which its position is characterized. Two teeth can have identical relative (%) CRes locations, but the M/F required for their translation will be different if their root lengths are different. (As noted previously, the M/F for translation is equal to the actual distance in millimeters between the force and the CRes.) Therefore,

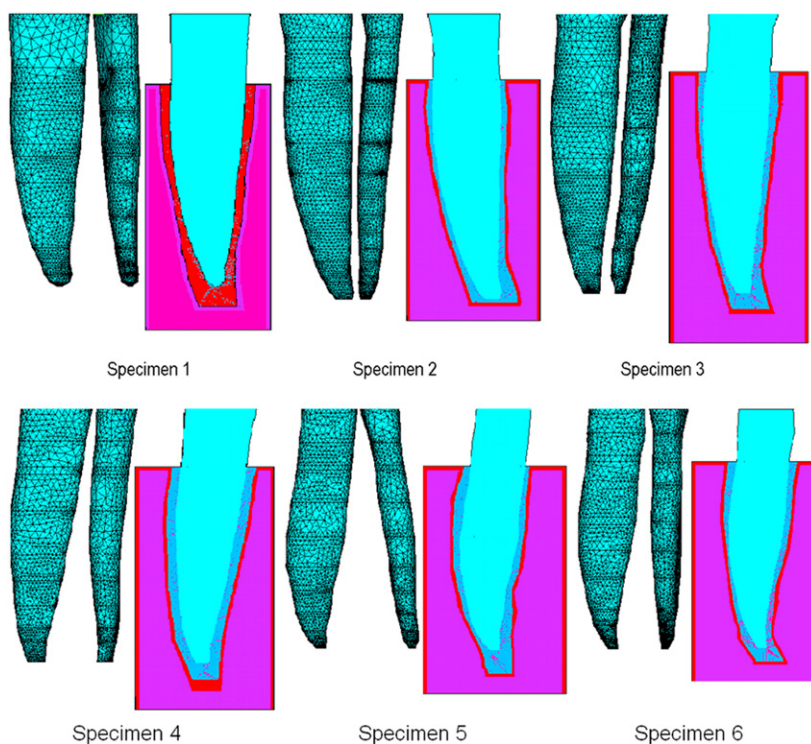


Fig 3. Six specimen models and root profiles.

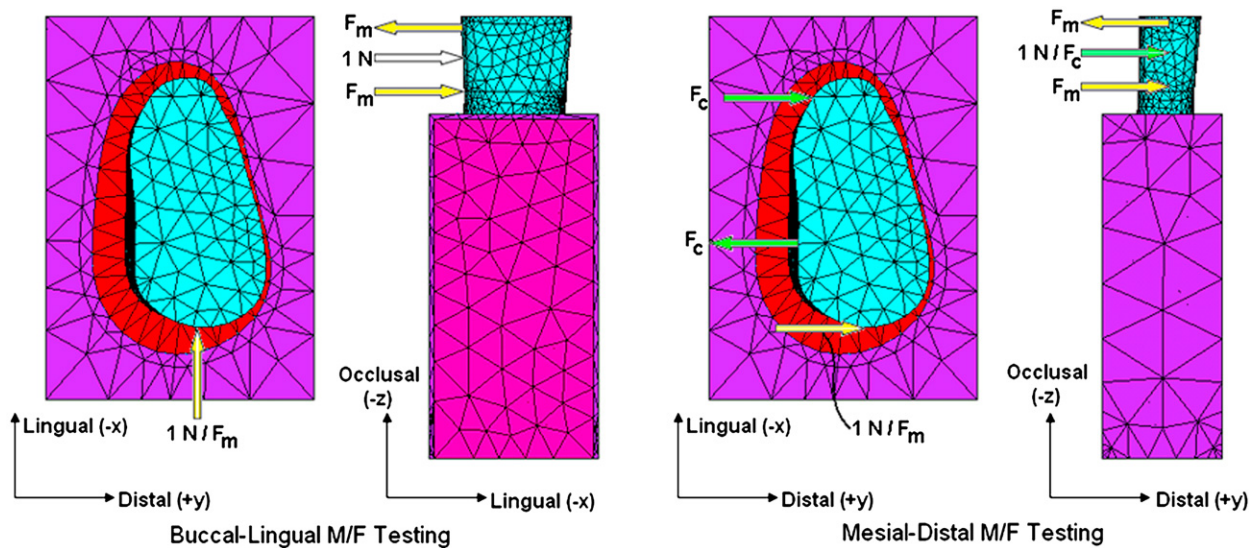


Fig 4. Loading conditions in BL and MD directions. The combination of the forces produces the desired M/F.

clinical determination of the CRes requires information of tooth length if the relative location is used.

It is instructive to examine the behavior observed herein by applying the 2 definitions of CRes. If, as an

example, only the BL force ($F_x = -1.0$ N) were applied to the bracket, the BL CRes (and the entire tooth) would displace by 0.0036 mm lingually (Fig 5). Because of the moment (M_y) produced by F_x about the CRes, the tooth

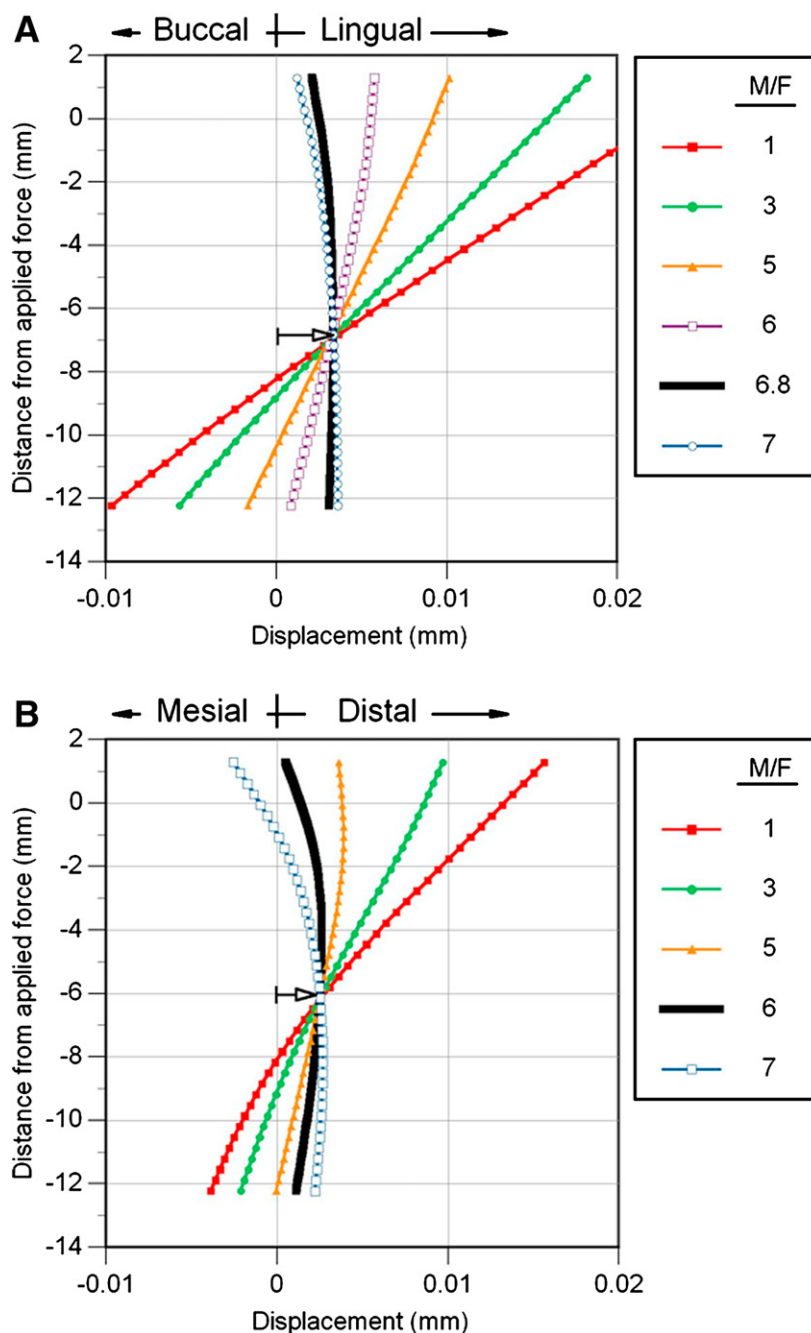


Fig 5. A, BL and B, MD displacements of the axial path with families of (A) M_y/F_x and (B) M_x/F_y . The most vertical *thick black line* is translation, and the associated M/F defines the location of CRes. *Open arrows* indicate displacements of CRes. Note that the horizontal and vertical axis scale differences (approximately 500/1) exaggerate the tooth bending deformations.

would also rotate (crown in, root apex out) about the displaced CRes. (At the CRes, the equivalent force-moment system of F_x acting on the bracket is equal to F_x plus the moment of the couple, \dot{M}_y .) Thus, the amounts of crown movement toward the lingual aspect that are

associated with CRes translation and tipping are additive. In contrast, root apex displacement is the net difference between the CRes lingual translatory displacement and the buccal movement of the apex because of rotation. This movement, uncontrolled tipping, is

Table IV. Locations of the CRes from the line of action of the force and as percentages of root length from the alveolar crest CRes translations

Specimen	Location (mm)		Translation of CRes (mm)	
	BL	MD	BL	MD
1	6.8 (46%)	6.2 (40%)	0.0036	0.0026
2	8.1 (45%)	6.7 (31%)	0.0026	0.0036
3	7.7 (43%)	6.6 (36%)	0.0016	0.0016
4	6.8 (44%)	6.0 (40%)	0.0043	0.0030
5	7.0 (48%)	6.1 (40%)	0.0030	0.0030
6	8.2 (51%)	7.0 (43%)	0.0030	0.0023
Mean	7.4* (46%)	6.4* (38%)	0.0030	0.0026
SD	0.65 (0.03%)	0.39 (0.04%)	0.0009	0.0007

*Statistical difference in the means.

characterized by a net buccal displacement of the root apex, indicating that rotation is the greater contributor to root tip deflection. In contrast, CRes displacement is entirely due to translation. (No matter where that $F_x = -1.0$ N is applied to the tooth, the CRes would translate 0.0033 mm toward the lingual aspect, but the amount, and possibly the direction, of rotation about the CRes would change because \dot{M}_y changes.) The moment (\dot{M}_y) produced by F_x about CRes is equal to the magnitude of F_x (1.0 N) times the (sought unknown) distance from the line of action of F_x (through the bracket) to the CRes. As an increasing counter (to \dot{M}_y) moment of a couple (M_y) is applied by the appliance, the amount of rotation about the CRes decreases. When M_y is sufficiently large to move the root apex back to its original position, it is described as controlled tipping. Net tooth rotation is eliminated when the moment applied by the appliance, M_y , is further increased so that its magnitude equals \dot{M}_y . That M_y/F_x corresponds to translation (ie, the most vertical displacement line), and it is the sought distance of the CRes from the bracket (Fig 5). (Appropriately, the unit of M/F is a length.) By increasing the magnitude of the appliance-generated M_y beyond \dot{M}_y , the crown tip can be rotated back to its original location. This is called pure root movement. The relationships between these amounts of translation and rotation are defined by the location of the CRes.

The results provide clear evidence that the location of the CRes changes with force direction. The CRes is a point in the plane shared by the force and displacement. A force acting on the CRes causes pure tooth translation in the plane. That takes into consideration the resistance from the tooth's supporting tissues, which depend also on the root shape that is perpendicular to the direction of movement. As the direction changes, so does the root shape, and hence the resistance to move-

ment and the CRes. Thus, as the direction of the force vector changes from tipping the tooth in 1 direction to the other, it might be useful to think of the CRes as morphing from 1 location to the next.

The observation that 6 similar specimens had a range of CRes locations and direction-dependent location differences clearly suggests that our specific numeric results should not be generalized to other types of teeth, although these root shapes resemble those of human mandibular central incisors much more so than they resemble human canines, for example.²¹ Furthermore, there are real and unmodeled confounding features (multiple roots, level of bone support, PDL thickness, root-bone proximity interactions, and homogeneous, isotropic, and elastic material behavior, and so on) that undoubtedly affect the locations of the CRes and the differences in their BL vs MD locations. But these nuances and assumptions affect the results in both directions of movement; thus, they are unlikely to produce conclusions contrary to the finding that there must be direction-dependent CRes location differences.

It is speculated, but worthy of additional study, that the location of the CRes (hence M/F for translation) would not be significantly affected if the magnitude of F_x were in the range that does not cause root-bone contact. On the other hand, the location of the CRes would change in a nonlinear way because of PDL anisotropy caused by the nonuniformly oriented and distributed fibers that provide resistance only in tension along their respective lengths. The matrix (modeled as isotropic and linear elastic) functions in compression and tension. Compared with functional loads, orthodontic forces are small, and, if it were not for the fibers, orthodontic strains and stresses in the matrix could be assumed to be linear.

CONCLUSIONS

In the mandibular central incisors of dogs, the appropriate M/F for translation in the BL direction is greater than in the MD direction. Thus, the BL CRes is located more apically than the MD CRes.

REFERENCES

1. Chen J, Katona TR. The limitations of the instantaneous centre of rotation in joint research. *J Oral Rehabil* 1999;26:274-9.
2. Schneider J, Geiger M, Sander FG. Numerical experiments on long-time orthodontic tooth movement. *Am J Orthod Dentofacial Orthop* 2002;121:257-65.
3. Bourauel C, Keilig L, Rahimi A, Reimann S, Ziegler A, Jäger A. Computer-aided analysis of the biomechanics of tooth movements. *Int J Comput Dent* 2007;10:25-40.
4. Cattaneo PM, Dalstra M, Melsen B. The finite element method: a tool to study orthodontic tooth movement. *J Dent Res* 2005;84:428-33.

5. Matsui S, Caputo AA, Chaconas SJ, Kiyomura H. Center of resistance of anterior arch segment. *Am J Orthod Dentofacial Orthop* 2000;118:171-8.
6. Sia S, Koga Y, Yoshida N. Determining the center of resistance of maxillary anterior teeth subjected to retraction forces in sliding mechanics. *Angle Orthod* 2006;77:999-1003.
7. Tanne K, Koenig HA, Burstone CJ. Moment to force ratios and the center of rotation. *Am J Orthod Dentofacial Orthop* 1988;94:426-31.
8. Yoshida N, Koga Y, Mimaki N, Kobayashi K. In vivo determination of the centres of resistance of maxillary anterior teeth subjected to retraction forces. *Eur J Orthod* 2001;23:529-34.
9. Yoshida N, Koga Y, Saimoto A, Ishimatsu T, Yamada Y, Kobayashi K. Development of a magnetic sensing device for tooth displacement under orthodontic forces. *IEEE Trans Biomed Eng* 2001;48:354-60.
10. Tanne K, Nagataki T, Inoue Y, Sakuda M, Burstone CJ. Patterns of initial tooth displacements associated with various root lengths and alveolar bone heights. *Am J Orthod Dentofacial Orthop* 1991;100:66-71.
11. Choy K, Pae EK, Park Y, Kim KH, Burstone CJ. Effect of root and bone morphology on the stress distribution in the periodontal ligament. *Am J Orthod Dentofacial Orthop* 2000;117:98-105.
12. Christiansen RL, Burstone CJ. Centers of rotation within the periodontal space. *Am J Orthod* 1969;55:353-69.
13. Vollmer D, Bourauel C, Maier K, Jager A. Determination of the centre of resistance in an upper human canine and idealized tooth model. *Eur J Orthod* 1999;21:633-48.
14. Yoshida N, Jost-Brinkmann PG, Koga Y, Mimaki N, Kobayashi K. Experimental evaluation of initial tooth displacement, center of resistance, and center of rotation under the influence of an orthodontic force. *Am J Orthod Dentofacial Orthop* 2001;120:190-7.
15. Jones ML, Hickman J, Middleton J, Knox J, Volp C. A validated finite element method study of orthodontic tooth movement in the human subject. *J Orthod* 2001;28:29-38.
16. Qian H, Chen J, Katona TR. The influence of PDL principal fibers in a 3-dimensional analysis of orthodontic tooth movement. *Am J Orthod Dentofacial Orthop* 2001;120:272-9.
17. Provatidis CG. A comparative FEM-study of tooth mobility using isotropic and anisotropic models of the periodontal ligament. Finite element method. *Med Eng Phys* 2000;22:359-70.
18. Auyeung L, Bouwsma OJ, Polson AM. Periodontal fiber attachment and apical root resorption. *Endod Dent Traumatol* 1988;4:219-25.
19. Natali AN, Pavan PG, Scarpa C. Numerical analysis of tooth mobility: formulation of a non-linear constitutive law for the periodontal ligament. *Dent Mater* 2004;20:623-9.
20. Chen J, Bulucea I, Katona TR, Ofner S. Complete orthodontic load systems on teeth in a continuous full archwire: the role of triangular loop position. *Am J Orthod Dentofacial Orthop* 2007;132:143. e141-8.
21. vanBeek GC. Dental morphology: an illustrated guide. 2nd ed. Bristol: United Kingdom; 1983. Butterworth-Heinemann.